

CROATICA CHEMICA ACTA
CCACAA **80** (2) 203–209 (2007)

ISSN-0011-1643
CCA-3161
Original Scientific Paper

Multicanonical Monte Carlo Calculation of the First-order Phase Transition of Lennard-Jones Fluids*

Chizuru Muguruma,^{a,**} Yuko Okamoto,^b and Masuhiro Mikami^c

^a*Faculty of Liberal Arts, Chukyo University, Toyota, Aichi 470-0393, Japan*

^b*Department of Physics, Graduate School of Science, Nagoya University, Furo-cho, Chikusa-ku, Nagoya, Aichi 464-8602, Japan*

^c*Research Institute for Computational Sciences, National Institute of Advanced Industrial Science and Technology, Tsukuba, Ibaraki 305–8568, Japan*

RECEIVED SEPTEMBER 30, 2006; REVISED MARCH 9, 2007; ACCEPTED MARCH 14, 2007

Keywords

- the multicanonical Monte Carlo method
 - first-order phase transition
 - liquid-solid phase transition
 - solid-solid phase transition
- a bulk Lennard-Jones fluid system
 - thermodynamic properties

The liquid-solid phase transition was investigated by the multicanonical Monte Carlo method for a bulk Lennard-Jones fluid system that consists of 256 argon particles. The reliability of the multicanonical weight factor we determined was confirmed by the flatness of the histogram obtained by the multicanonical Monte Carlo production run. The first-order phase transition between solid and liquid phase was observed around 130 K from the change in thermodynamic properties as a function of temperature. Besides, the small change between two solid structures was also observed at 60 K from the radial distribution function, from the heat capacity and from conventional canonical Monte Carlo calculation at 60 K. Neither of them is not f. c. c. structure which is known as the most stable.

INTRODUCTION

Conventional canonical simulations of complex systems tend to get trapped at low temperatures in local minimum states on the potential energy surface. The multicanonical (MUCA) algorithm^{1,2} has been introduced in order to overcome this multiple-minima problem and has been applied to study first-order phase transitions^{1–14} (for recent reviews, see Refs. 15 and 16). The algorithm is based on an artificial, non-Boltzmann weight factor and performs a free one-dimensional random walk in potential energy space, which allows the simulation to avoid getting trapped in states of energy local minima. Moreover, one can calculate the expectation values of thermodyna-

mic quantities as functions of temperature by applying the single-histogram reweighting techniques¹⁷ to the results of one long production run. A Lennard-Jones fluid system, such as an argon fluid, is one of typical systems with first-order phase transitions.^{7,10,18,19} In the present study, we apply the MUCAMC method to the bulk argon system and investigate the changes in thermodynamic quantities across the phase transition point.

This article is organized as follows. In section *Computational Methods*, the MUCAMC method is briefly described. We report the results of the MUCAMC simulation of a bulk argon system in section *Results and Discussion*. Conclusions follow in section *Concluding Remarks*.

* Dedicated to Professor Haruo Hosoya in happy celebration of his 70th birthday.

** Author to whom correspondence should be addressed. (E-mail: muguruma@lets.chukyo-u.ac.jp)

COMPUTATIONAL METHODS

Multicanonical Ensemble

Although the multicanonical algorithm is explained in detail elsewhere,^{14–16} we give a short overview in this subsection for completeness. In the canonical ensemble, the probability distribution of the potential energy E , $P_B(E;T)$, is given by the product of the density of states $n(E)$ and the Boltzmann weight factor $W_B(E;T)$:

$$P_B(E;T) \propto n(E)W_B(E;T) = n(E)e^{-\beta E} \quad (1)$$

where β is the inverse temperature $1/k_B T$ with the Boltzmann constant k_B and temperature T . Because $n(E)$ is a rapidly increasing function and $W_B(E;T)$ decreases exponentially, $P_B(E;T)$ generally has a bell-like shape.

In multicanonical ensemble each state is weighted by a non-Boltzmann weight factor $W_{\text{mu}}(E)$, which we refer to as the multicanonical weight factor, so that a uniform potential energy distribution may be obtained:

$$P_{\text{mu}}(E) \propto n(E)W_{\text{mu}}(E) \equiv \text{constant} \quad (2)$$

The flat artificial energy distribution implies that a one-dimensional free random walk in the potential energy space is realized. The random walk allows the system to escape from any local-minimum-energy states and to sample the configurational space much more widely with a smaller number of simulation steps than the conventional canonical Monte Carlo or molecular dynamics methods.

From the definition in Eq. (2), the multicanonical weight factor $W_{\text{mu}}(E)$ is inversely proportional to the density of the states $n(E)$ and can be written as follows:

$$W_{\text{mu}}(E) \equiv e^{-S(E)/k_B} = \frac{1}{n(E)} \quad (3)$$

where $S(E)$ is the entropy in the microcanonical ensemble:

$$S(E) = k_B \ln n(E) \quad (4)$$

Since the density of states of the system is usually unknown, the multicanonical weight has to be determined numerically by iterations of short preliminary runs. In the present study, we employ the iterative procedure in Ref. 20 and single- and multiple-histogram reweighting techniques (see Ref. 19 for details).

A multicanonical Monte Carlo simulation is performed, for instance, with the usual Metropolis criterion.²¹ The transition probability of state x with potential energy E to state x' with potential energy E' is given by

$$w(x \rightarrow x') = \begin{cases} 1, & \text{for } \Delta S \leq 0, \\ \exp(-\Delta S/k_B), & \text{for } \Delta S > 0, \end{cases} \quad (5)$$

where

$$\Delta S \equiv S(E') - S(E) \quad (6)$$

Once the multicanonical weight factor (equivalently the entropy $S(E)$) is given, one performs a long multicanonical production run. By tracing the potential energy surface during the simulation, the global-minimum energy state can be identified. Moreover, the expectation value of a physical quantity Q at any temperature T ($= 1/k_B\beta$) is given by

$$\langle Q \rangle_T = \frac{\sum_E Q(E)n(E)e^{-\beta E}}{\sum_E n(E)e^{-\beta E}} \quad (7)$$

where the optimal density of states $n(E)$ is obtained by the single-histogram reweighting techniques¹⁷ (see Eq. (2)):

$$n(E) = \frac{H_{\text{mu}}(E)}{W_{\text{mu}}(E)} \quad (8)$$

and $H_{\text{mu}}(E)$ is the recorded histogram of the probability distribution of potential energy $P_{\text{mu}}(E)$ in the production run.

Computational Details

We put 256 argon particles in a cubic cell with periodic boundary conditions. The edge size is fixed at 21.75 Å so that the density of the system is 1.65 g cm⁻³, which corresponds to the density of solid argon at 40.15 K. A pair of argon particles with distance r_{ij} interacts through the Lennard-Jones pair potential

$$v(r_{ij}) = 4\epsilon \left[\left(\frac{\sigma}{r_{ij}} \right)^{12} - \left(\frac{\sigma}{r_{ij}} \right)^6 \right] \quad (9)$$

where the potential parameters of argon are $\epsilon = 0.9961$ kJ/mol and $\sigma = 3.405$ Å,²² and the total potential energy per particle of the system that consists of N argon particles is given by

$$E = \frac{1}{N} \sum_{i=1}^{N-1} \sum_{j>i}^N v(r_{ij}). \quad (10)$$

The interactions of all particles are truncated at a distance of $r_c = 10.88$ Å which corresponds to a half length of the edge size. The multicanonical weight factor was determined for the temperature range $T \leq 200$ K. Thermodynamic quantities are calculated by the reweighting techniques in Eqs. (7) and (8). For instance, the pressure P and heat capacity C_V are calculated from the following equations:

$$P = \frac{Nk_B T}{V} + \frac{1}{3V} \sum_{i=1}^{N-1} \sum_{j>i}^N r_{ij} f_{ij} \quad (11)$$

$$C_v = N^2 \frac{\langle E^2 \rangle_T - \langle E \rangle_T^2}{k_B T^2} \quad (12)$$

where f_{ij} is the pair force acting on atom i due to atom j and V is the volume of the system. The potential energies and pressures are corrected by the following equations:

$$E_c = \frac{8}{9} \pi \sigma^3 \rho \varepsilon \left\{ \left(\frac{\sigma}{r_c} \right)^9 - 3 \left(\frac{\sigma}{r_c} \right)^3 \right\} \quad (13)$$

$$P_c = \frac{16}{9} \pi \sigma^3 \rho^2 \varepsilon \left\{ 2 \left(\frac{\sigma}{r_c} \right)^9 - 3 \left(\frac{\sigma}{r_c} \right)^3 \right\} \quad (14)$$

where ρ is the number density of the system.

One MC sweep is defined to consist of 256 coordinate updates of a randomly chosen particle with the Metropolis evaluation for each update. Since we found the phase transition-like behavior in lower energy region around for higher energy region -7.3 kJ/mol, the MUCAMC production run was performed by dividing two energy regions: one is from -7.2 to -5.3 kJ/mol and another is below -6.7 kJ/mol. The phase transition takes place between two phases within these energy regions. Total number of MC sweeps for the MUCAMC production run was 3×10^8 for higher energy region and 2×10^7 for lower energy region. The conventional canonical MC calculation with the same condition was also performed at 40 K, 60 K, 80 K, 110 K, and 200 K to compare the expectation values for physical quantities with those of the MUCAMC calculation. All calculations were performed with our own computer code.

RESULTS AND DISCUSSION

Reliability of the MUCA Weight Factor

We first examine how the present MUCAMC production run performed. In an ideal MUCAMC production run, we should obtain a uniform potential energy distribution and observe a free random walk in the potential energy space covering the entire energy range of interest. Figure 1 is the entropy $S(E)$ which calculated from the multicanonical weight factor $W(E)$. In the present study, the multicanonical weight factor for the temperature range $T \leq 200$ K is determined by setting $S(E) = 0$ at $E = -7.8$ kJ/mol.

Figure 2(a) shows the time series of the total potential energy per particle from the MUCAMC production run of higher energy region and Figure 2(b) shows those from the conventional canonical MC calculation at 80 K and 200 K. To avoid simulating the energy below -7.2 kJ/mol, $\Delta S(E)$ is fixed at $\Delta S(E)$ at $E \leq -7.2$ kJ/mol for

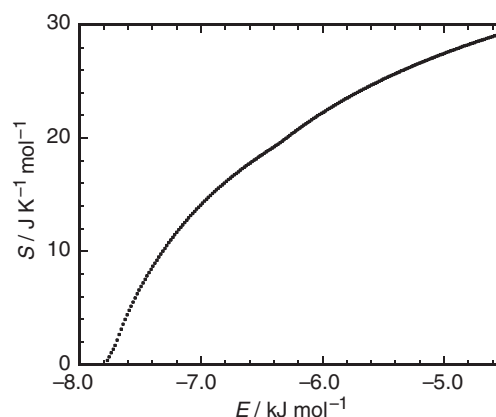


Figure 1. The entropy $S(E)$ which calculated from the multicanonical weight factor by the relation $S(E) = -k_B \ln W(E)$. We have set the value of entropy to zero at $E = -7.8$ kJ mol $^{-1}$.

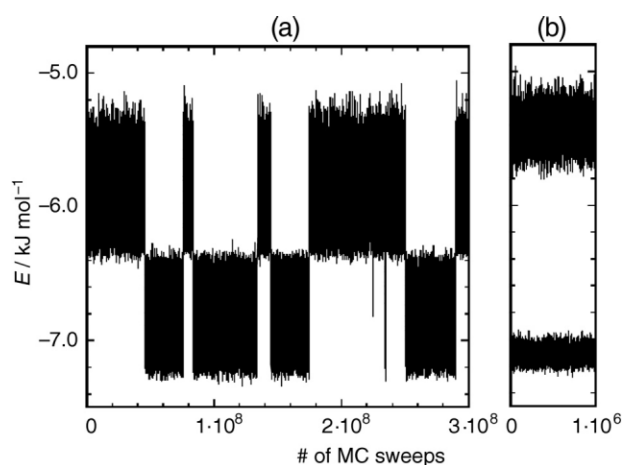


Figure 2. Time series of total potential energy per particle that was obtained by (a) a long production run of the MUCAMC simulation above -7.2 kJ mol $^{-1}$ and (b) and the conventional canonical MC calculations at temperatures 80 and 200 K.

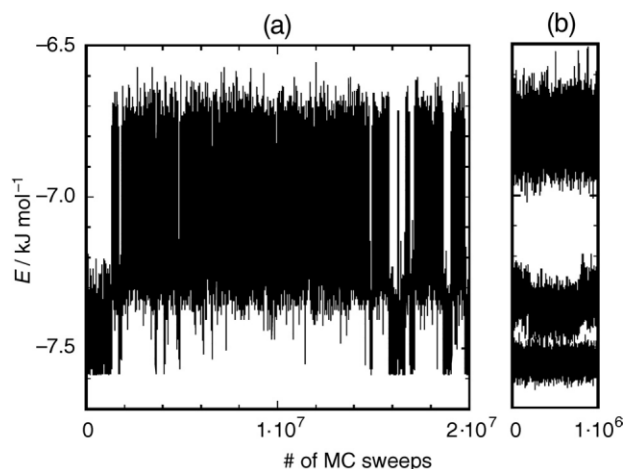


Figure 3. Time series of total potential energy per particle that was obtained by (a) a long production run of the MUCAMC simulation below -6.7 kJ mol $^{-1}$ and (b) and the conventional canonical MC calculations at temperatures 40 K, 60 K and 110 K.

$E = -7.2$ kJ/mol during the MUCAMC production run. We indeed see random walks between from -5.3 kJ/mol to -7.2 kJ/mol. However the random walks are not completely free and the energy regions are divided into two parts whose boundary is located around -6.3 kJ/mol. Within both energy regions we have free random walks, but the transition between the two regions took place only eight times during the production run. This implies that the MUCA weight factor was accurately determined in the entire energy range between -7.2 kJ/mol and -5.3 kJ/mol except near -6.3 kJ/mol. In Figures 3(a) and (b), the time series of the total potential energy per particle from the MUCAMC production run below -6.7 kJ/mol and from the conventional canonical MC calculation at 40 K, 60 K and 110 K are shown. To avoid simulating the energy above -6.7 kJ/mol, $\Delta S(E)$ is fixed at $\Delta S(E)$ at $E = -6.7$ kJ/mol for $E \leq -6.7$ kJ/mol during the MUCAMC production run. As well as Figures. 2(a) and (b), we can see free random walks between -7.2 kJ/mol and -5.4 kJ/mol except near -7.4 kJ/mol.

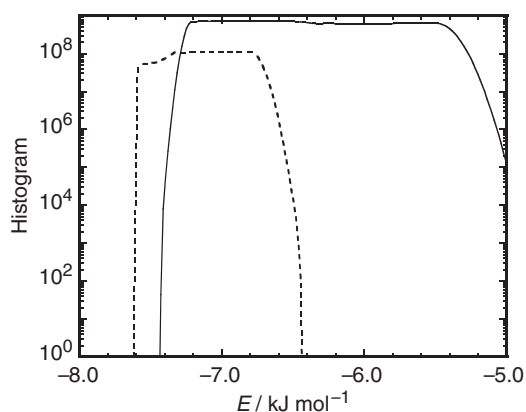
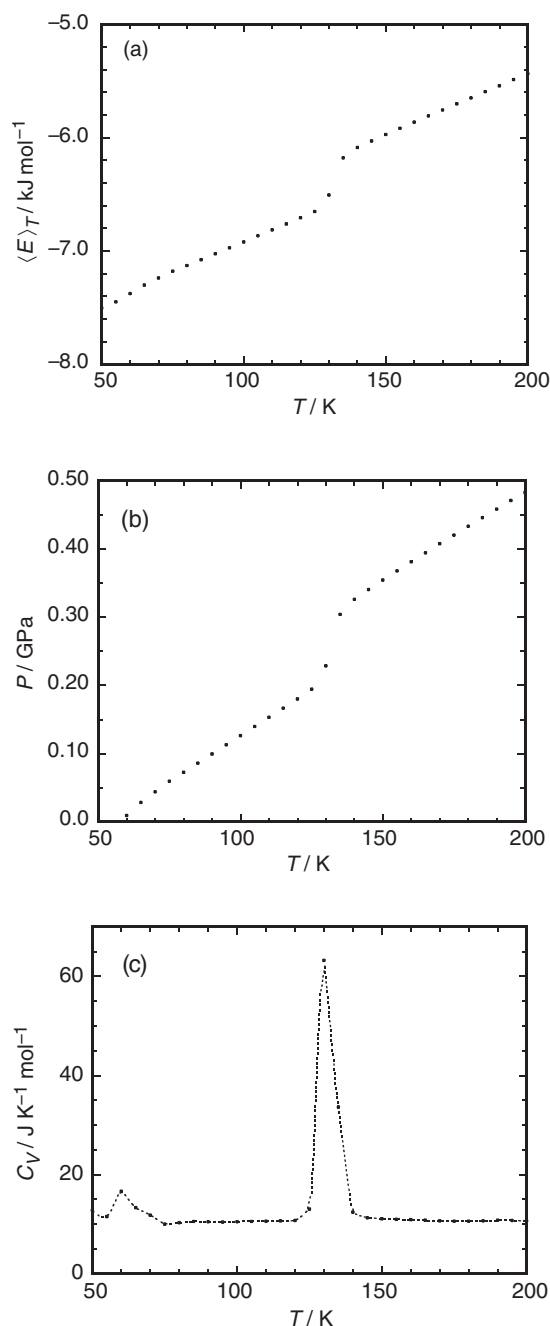


Figure 4. Histograms of the total potential energy per particle that were obtained by the MUCAMC production runs. The solid line stands for that obtained by the MUCAMC production run above -7.2 kJ mol $^{-1}$ and the dashed line stands for that obtained by the MUCAMC production run below -6.7 kJ mol $^{-1}$.

Figure 4 is the histograms of the potential energy distribution that were obtained by two MUCAMC production runs. We observe flat histograms between -7.2 kJ/mol and -5.4 kJ/mol for higher energy region and between -7.6 kJ/mol and -6.7 kJ/mol for lower energy region. This appears to imply that the multicanonical ensemble is realized in the entire potential energy range. If we examine Figure 4 carefully, however, we find two uniform distributions with slightly different heights below and above -6.4 kJ/mol for the production run of the higher energy region, and also below and above -7.4 kJ/mol for the production run of the lower energy region for each histograms. This implies that the MUCA weight factor was accurately determined in the entire energy range between -7.6 kJ/mol and -5.3 kJ/mol

Expectation Values of Thermodynamic Quantities

We now examine thermodynamic quantities as functions of temperature. We calculated expectation values at every 5 K from 50 K to 200 K by applying the reweighting techniques in Eqs. (7) and (8) to the results of two MUCAMC production runs. Average potential energy per particle, pressure, heat capacity, entropy, and Helmholtz free energy are shown in Figure 5. As we will be shown in detail below, we find that all these data suggest that there exist a phase transition at $T = 130$ K in the present system and imperceptible transition at $T = 60$ K. The phase transition at 130 K is considered to be the liquid-solid transition.



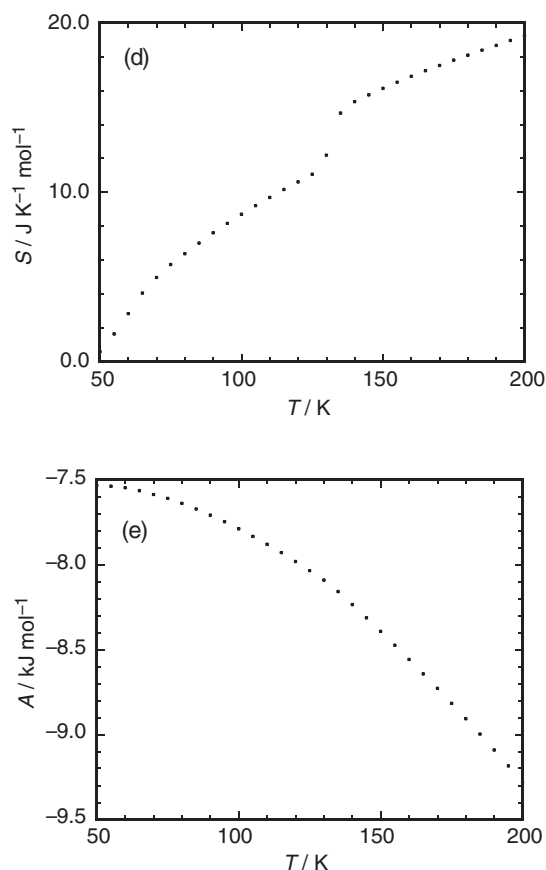


Figure 5. The thermodynamic properties (a) average total potential energy per particle, (b) pressure, (c) heat capacity, (d) entropy, and (e) Helmholtz free energy obtained from the MUCAMC production run by the reweighting techniques. The expectation values were calculated at each 5 K from 50 K to 200 K.

The average total potential energy per particle is shown in Figure 5(a). The energy range from -7.2 kJ/mol to -5.4 kJ/mol and from -7.6 kJ/mol to -6.7 kJ/mol corresponds to the temperature range from 70 K to 200 K and from 50 K to 110 K, respectively. The sudden change in the average energy suggests that there exists a phase transition around $T = 130$ K. A similar behavior is also observed for the 108 argon system, but the transition temperature is by about 20 K higher than the present system.

The pressure, shown in Figure 5(b), also shows the sudden change at 130 K, which agrees well with the experimental fact that the melting point of solid argon is about 130 K under the corresponding pressure of 0.3 GPa.²³ Thus, the phase transition observed in the present simulation seems to be the liquid-solid phase transition. We will confirm this below in Figure 6. This can be interpreted by the fact that the solid state obtained in the simulation of the 108 argon system is more crystal-like (and lower in pressure) than that obtained in the present simulation, judging from the radial distribution functions in Figure 7.

Heat capacity is shown in Figure 5(c). A significant peak is observed at 130 K in the present system and that

at 150 K in the 108 argon system. We see that the width and the height of the peak becomes narrower and higher, respectively, in the present system than in the 108 argon system, which are typical behaviors of heat capacity as the number of particles is increased.

Calculating entropy by the ordinary molecular simulation methods requires a lot of efforts. However, the entropy $S(E)$ in the microcanonical ensemble can be easily obtained by the multicanonical algorithm. The entropy in the canonical ensemble at temperature T can then be calculated by the reweighting techniques as follows:

$$S(T) = \frac{\sum_E S(E)n(E)e^{-\beta E}}{\sum_E n(E)e^{-\beta E}}. \quad (15)$$

The results are shown in Figure 5(d). The phase transition is again recognized in the figure. We remark that the differences in energy 0.50 kJ/mol (Figure 5(a))

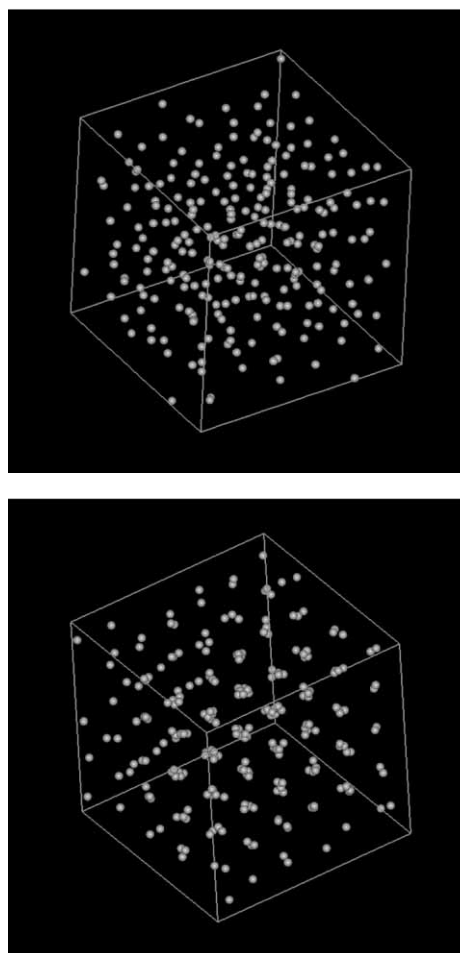


Figure 6. Snapshots obtained by the MUCAMC production run. The total potential energy is (a) -5.75 kJ mol $^{-1}$, and (b) -6.75 kJ mol $^{-1}$, respectively. Pictures are the projection along a crystal axis. The mass of argon particles are observed in the snapshot (b) because of the fluctuation.

and in entropy $3.62 \text{ J K}^{-1} \text{ mol}^{-1}$ (Figure 5(d)) at the phase transition temperature 130 K almost satisfy the thermodynamic relation $\Delta S = \Delta E / T$ (3.62 versus 3.85).

Helmholtz free energy is also one of the physical quantities that are difficult to calculate by the ordinary computer simulation methods. In the multicanonical algorithm, we can calculate the Helmholtz free energy by the relation $A(T) = \langle E \rangle_T - TS(T)$. It is shown in Figure 5(e). We observe a slight change in slope is again observed at 130 K in the present system.

Structure Analyses

Snapshots obtained from the MUCAMC production run are shown in Figure 6. In the higher energy state of Figure 6(a), argon particles are scattered randomly, whereas argon particles are almost regularly arranged in the lower energy state of Figure 6(b). Therefore we confirm that the high-energy state correspond to the liquid state and the low-energy state to the solid state.

The radial distribution functions (RDFs) are calculated for the conventional canonical MC calculation by the following equation:

$$g(R) = \frac{1}{4\pi R^2 \Delta R} \frac{V}{N(N-1)} \left\langle \sum_{i=1}^N \Delta N_i(R) \right\rangle \quad (16)$$

where N is the number of particles included in the system whose volume is V , and $\Delta N_i(R)$ is average number of particles included between two spheres whose distances are R and $R+\Delta R$ from particle i . RDFs can be also calculated by applying the reweighting techniques in Eqs. (7) and (8) to $\Delta N_i(R)$ obtained by the MUCAMC production run.

Figure 7 shows the RDFs at 100 K, 130 K, and 150 K. RDF at 150 K shows that the system is in liquid state

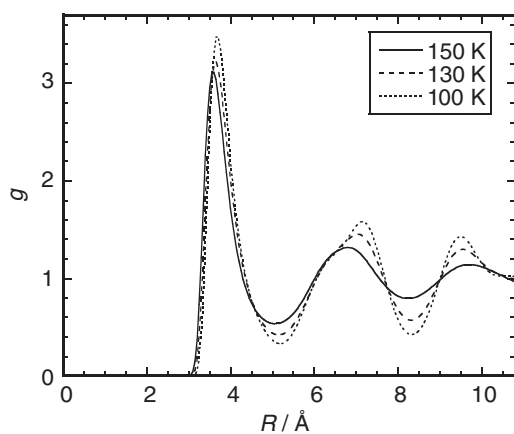


Figure 7. The argon-argon radial distribution function g at $T = 100 \text{ K}$, 130 K , and 150 K , which were obtained from the MUCAMC production run by the reweighting technique. The solid line stands for that at 150 K , the dashed line stands for that at 100 K , and the dotted line stands for that at 130 K of the system of 256 argon particles.

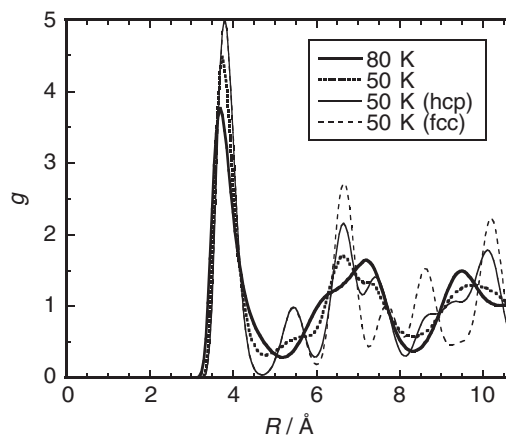


Figure 8. The argon-argon radial distribution function g at $T = 50 \text{ K}$ and 80 K . The thick solid line stands for that at 80 K and the thick dotted line stands for that at 50 K of the system of 256 argon particles, which were obtained from the MUCAMC production run by the reweighting technique. The thin solid line stands for that at 50 K of the system of 384 argon particles (h. c. p. structure) and the thin dashed line stands for that at 50 K of the system of 256 argon particles (f. c. c. structure), which were obtained from the conventional canonical MC calculations.

because the curvature changes gradually. As the temperature is lower, the second peak at 6.3 \AA of liquid state is split into 6.2 \AA and 7.2 \AA , and the third peak becomes closer. Argon particles in the system are more structured at 100 K than at 150 K . The curvature of RDF at 130 K is intermediate between those at 100 K and 150 K .

In order to investigate the structural change in lower energy region, RDF at 50 K is compared with that at 80 K . At 50 K , small peak is appeared at 5.7 \AA and the peak at 6.6 \AA becomes higher than that at 7.2 \AA . But the total potential energy per particle alternates between higher energy state and lower energy state in the time series of the conventional canonical MC calculation at 60 K during the same canonical simulation (see Figure 3(b)). This indicates that the structural phase transition takes place between two energy states with small energy barrier.

To analyze the structures obtained by the MUCAMC production run below -6.7 kJ/mol , the RDFs are calculated for the face center cubic (f. c. c.) structure and the hexagonal closed packing (h. c. p.) structure from the structures obtained by the conventional canonical MC calculation. We put 256 argon particles in a periodic cubic cell of 21.75 \AA edge for f. c. c. structure and put 384 argon particles in a periodic orthorhombic cell of $23.07 \text{ \AA} \times 26.64 \text{ \AA} \times 25.12 \text{ \AA}$ for h. c. p. structure. The RDF at 50 K shows different position and height of the peaks from that of f. c. c. structure, but shows similar in position of the peaks to that of h. c. p. structure. Though the system size seems to be not fit to the crystal structure, two energy states obtained by the MUCAMC production run below -6.7 kJ/mol are the semi-stable states and lower energy state might belong to the h. c. p. structure.

CONCLUDING REMARKS

The MUCAMC method was applied to the 256 bulk argon system. The histogram of energy distribution obtained from the multicanonical production run tells that the multicanonical weight factor that we determined was reliable for the energy range between -7.6 kJ/mol and -5.4 kJ/mol, which corresponds to the temperature range from 50 K to 200 K from the average total potential energy. The expectation values of physical quantities indicated that the phase transition between liquid and solid states is observed around 130 K. We are further investigating the relationship between structures and thermodynamic quantities among face center cubic structure, hexagonal closed packing structure, and two solid structures obtained in the present study.

Acknowledgements. – Chizuru Muguruma and Yuko Okamoto were supported, in part, by the Ministry of Education, Culture, Sports, Science and Technology (MEXT), Japan: Chizuru Muguruma by Grants-in-Aid for Young Scientists (B), Grant No. 16740244 and Yuko Okamoto by Grants-in-Aid for the Next Generation Super Computing Project, Nanoscience Program and for Scientific Research in Priority Areas, Water and Biomolecules.

REFERENCES

1. B. A. Berg and T. Neuhaus, *Phys. Lett.* **B267** (1991) 249–253.
2. B. A. Berg and T. Neuhaus, *Phys. Rev. Lett.* **68** (1992) 9–12.
3. B. A. Berg and T. Celik, *Phys. Rev. Lett.* **69** (1992) 2292–2295.
4. U. H. E. Hansmann and Y. Okamoto, *J. Comput. Chem.* **14** (1993) 1333–1338.
5. Y. Okamoto and U. H. E. Hansmann, *J. Phys. Chem.* **99** (1995) 11276–11287.
6. W. Janke and S. Kappler, *Phys. Rev. Lett.* **74** (1995) 212–215.
7. N. B. Wilding, *Phys. Rev. E* **52** (1995) 602–611.
8. B. A. Berg and W. Janke, *Phys. Rev. Lett.* **80** (1998) 4771–4774.
9. K. K. Bhattacharya and J. P. Sethna, *Phys. Rev. E* **57** (1998) 2553–2562.
10. H. Liang and H. Chen, *J. Chem. Phys.* **113** (2000) 4469–4471.
11. C. Muguruma, Y. Okamoto, and M. Mikami, *Internet Electron. J. Mol. Des.* **1** (2002) 1–9.
12. B. A. Berg, *Comp. Phys. Commun.* **14** (2002) 52–57.
13. E. Bittner, W. Janke, and D. B. Saakian, *Phys. Rev. E* **67** (2003) 016105.
14. B. A. Berg, *Comp. Phys. Commun.* **153** (2003) 397–406.
15. B. A. Berg, *Fields Institute Communications* **26** (2000) 1–24; cond-mat/99009236.
16. A. Mitsutake, Y. Sugita, and Y. Okamoto, *Biopolymers (Peptide Science)* **60** (2001) 96–123.
17. (a) A. M. Ferrenberg and R. H. Swendsen, *Phys. Rev. Lett.* **61** (1988) 2635–2638; (b) *ibid.* **63** (1989) 1195–1198.
18. A. Rytönen, S. Valkealahti, and M. Manninen, *J. Chem. Phys.* **108** (1998) 5826–5832.
19. C. Muguruma, Y. Okamoto, and M. Mikami, *J. Chem. Phys.* **120** (2004) 7557–7563.
20. B. A. Berg, *Nuclear Physics B (Proc. Suppl.)* **63A–C** (1998) 982–984.
21. N. Metropolis, A. W. Rosenbluth, M. N. Rosenbluth, A. H. Teller, and E. Teller, *J. Chem. Phys.* **21** (1953) 1087–1092.
22. G. C. Maitland, M. Rigby, E. B. Smith, and W. A. Wakeham, *Intermolecular Forces: Their Origin and Determination*, Clarendon Press, Oxford, 1981.
23. F. Datchi, P. Loubeyre, and R. LeToullec, *Phys. Rev. B* **61** (2000) 6535–6546.

SAŽETAK

Multikanonski Monte Carlo proračuni faznog prijelaza prvog reda za Lennard-Jonesove fluide

Chizuru Muguruma, Yuko Okamoto i Masuhiro Mikami

Primjenom multikanonske Monte Carlo metode proučavan je fazni prijelaz čvrsto-tekuće za Lennard-Jonesov fluid od 256 čestica argona. Pouzdanost multikanonskog težinskog faktora potvrđena je ravnomjernošću histograma dobivenog kroz više ciklusa multikanonskog Monte Carlo proračuna. Iz promjena termodinamičkih svojstava s temperaturom izračunato je da se fazni prijelaz čvrsto-tekuće prvog reda događa na oko 130 K. Osim toga je na osnovu poznavanja funkcija radijalne raspodjele, toplinskog kapaciteta i provedenog standardnog kanonskog Monte Carlo proračuna utvrđeno da se na 60 K događa fazni prijelaz čvrsto-čvrsto između dviju struktura od kojih nijedna nije poznata stabilna f.c.c. struktura.